Bi-axial Seismic Activation of Civil Engineering Structures Equipped with Tuned Liquid Column Dampers

M. Reiterer[1] and F. Ziegler[2]

1. Department of Civil Engineering, Vienna University of Technology, Vienna, Austria,
   email: mr@allmech.tuwien.ac.at
2. Department of Civil Engineering, Vienna University of Technology, Vienna, Austria,
   email: franz.ziegler@tuwien.ac.at

ABSTRACT: *Tuned liquid column dampers (TLCD) considerably increase the effective damping of vibration prone civil engineering structures in horizontal motion. A single-degree-of-freedom (SDOF) basic system with a TLCD attached is analyzed under horizontal and vertical base excitations in order to prove its sensitivity with respect to the vertical parametrical forcing. The main result is cast in a sufficient condition for the linearized damping coefficient of the fluid motion to ensure its stability under the most critical, time harmonic forcing conditions. The output of computer simulations when varying the damping of the TLCD tuned with respect to frequency only, are verified experimentally by means of a novel model setup. The scaled Friuli 1976 earthquake is applied horizontally and vertically to an SDOF-shear frame with optimally tuned TLCD. A three-DOF-benchmark structure, equipped with two passive TLCD in parallel connection, optimally fine-tuned in state space, is analyzed by nonlinear computer modeling. Two different relevant earthquakes are alternatively applied in both, horizontal and vertical directions. In all cases it is verified, that sealed TLCD, (with the air-spring effect taken into account) are stable, since the optimal linear damping coefficient exceeds by far the required cut-off value of parametric resonance: the vertical component of the earthquake load remains ineffective. Hence, taking into account this sufficient condition with the maximum vertical ground (floor) acceleration assigned and the maximum amplitude of the fluid motion estimated, saves the consideration of the vertical seismic activation at all.*

Keywords: Vibration absorber; Horizontal-; Vertical excitations; Parametric resonance; Cut-off damping; Bernoulli equation; Tuned mass damper (TMD)-analogy; Den Hartog tuning; State space optimization

1. Introduction

Newly developed lightweight building materials and sophisticated numerical algorithms allow the design of tall and highly flexible civil engineering structures. These structures are vulnerable to dynamic loads, such as wind gusts or earthquakes. Hence, the mitigation of structural vibrations has been a major concern amongst structural engineers. One of the effective means to reduce the dynamic response is the application of dynamic vibration absorbers. The tuned mechanical damper, *TMD*, is one of the most popular passive control systems and has been broadly studied and applied to many engineering structures [1]. Its substitution by the innovative tuned liquid column damper, *TLCD*, which has been developed to the practical design stage during the last decade, see [2-6], is most promising. *TLCD* is a damping device in the extremely low frequency range that relies on the motion of a liquid mass in a rigid U-shaped tube. Its range of applicability can be extended to about 4.0 to 5.0*Hz*, if the air spring effect in the sealed U-shaped

tube is utilized. For extremely low frequencies, however, the air chambers are connected and air can flow freely to balance the pressure. The motion of the main system (of the relevant floor of the building) induces a phase-delayed relative motion of the liquid mass and, hence, interaction forces (and moments) to counteract the external force. Furthermore, a built-in orifice plate may become necessary, to induce additional turbulent damping and dissipation of kinetic energy in a controlled manner. For optimal tuning of the *TLCD* the natural circular frequency ω_A and the linearized damping coefficient ζ_A have to be suitably chosen, in analogy to the conventional *TMD*, for the latter see Den Hartog [7]. Computationally, the tuning of the *TLCD* is always performed in two steps. At first, the linearized computer model is tuned with respect to a selected mode of the main system using the simple analogy to *TMD*-tuning. Hochrainer [5] extensively discussed this simplifying step. Subsequent improvements of the performance in an *MDOF*-system are achieved by considering the neighboring modes as well in the state space representation, by minimizing the weighted squared area of the frequency response function, see again [5]. The second fine-tuning renders the optimal parameters quickly when Den Hartog's parameters are selected for the initial values of the numerical search process. Slightly modified parameters result, and, e.g., two *TLCD* in parallel connection, counteracting a single selected mode, turn out with different tuning parameters. This second step leads to an increase in the robustness of the proposed damping device. Final adjustments are easily performed in the course of in-situ testing. The *TLCD* ideally suited to excite the main structure in a controlled manner to measure its basic frequency, which enters in-situ fine tuning. In many respects *TLCD* exceed by far the capabilities of other vibration absorbing devices. Their main advantages comprise of low cost of design and maintenance, easy application to new buildings or in retrofitting existing structures, little additional mass since water is stored in buildings for fire protection or water supply and a simple tuning mechanism since the natural frequency and damping ratio can be adjusted by pressurizing the air chambers, adjusting their volume, and selecting a proper orifice plate.

While tuned liquid dampers (*TLD*) based on the sloshing fluid in the moving container are applied as well to reduce the vibrations at a well separated frequency, their reaction to disturbances is found rather uncontrolled, contrary the sealed tuned liquid column damper (*TLCD*) is self controlling to overloads and the fluid motion is controlled in any respect.

Most scientific work concentrated on the suppression of horizontal motions of structures also in case of earthquake activation and neglected the vertical component. Hence, the objective of this study is to develop a more general model of civil engineering structures with passive *TLCD* attached and to investigate any unwanted influence of the vertical seismic activation on the damping characteristics of *TLCD*. It has to be mentioned that parametric resonance also exists for the conventional pendulum type *TMD* whose point of suspension moves vertically, see, eg., Ziegler [8]. In order to prevent parametric resonance even under the most critical conditions of time harmonic excitation, a sufficient condition for the linearized damping coefficient of the *TLCD* is derived. Various computer models of optimally and sub optimally damped *TLCD* attached to an *SDOF*-shear frame, are investigated to study the sensitivity with respect to the vertical excitation. The outcome of the analysis is verified experimentally using a newly designed model set up. In addition to time harmonic forcing under the most critical conditions of parametric resonance, the scaled Friuli 1976 earthquake is applied assuming one and the same intensity in both directions. The experimental results agree well with the computational simulations. The cut-off damping coefficient of parametric resonance was verified. Finally, a three-*DOF*-structure, based on the benchmark definition paper by Spencer et al [9], is equipped with two passive optimally tuned *TLCD* in parallel connection on top of the building. Fine-tuning is performed in state space. Both seismograms, the *N-S* Friuli earthquake and the *N-S El* Centro 1940 earthquake, are applied in horizontal and vertical directions. Theoretical and experimental investigations indicate that the vertical component of the earthquake loading influences more or less the *TLCD* dynamics. However, it is verified, that in case of sealed *TLCD*, the common values of the optimal damping ratio are much larger than the very small cut-off damping coefficient, and thus, no undesired worsening effects are observed. Hence, after verifying the sufficient condition to prevent parametric resonance for the most critical case, the vertical component of any earthquake load must not be considered any further.

2. Basic System: SDOF-Shear Frame with TLCD Attached

Modal tuning of a *TLCD* when attached to an *MDOF*-structure can be approximately reflected by the interaction of an *SDOF*-shear frame with a *TLCD* on top. Substructure synthesis is applied and illustrated in Figure (1).
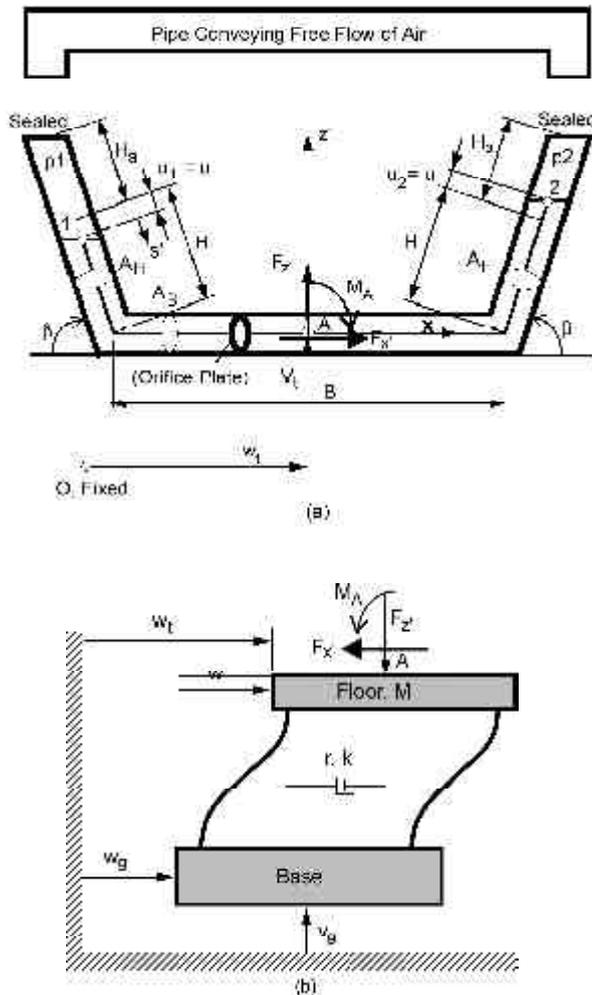
Figure 1. (a) Symmetrically shaped TLCD under combined horizontal and vertical floor excitations. When sealed, air chamber volume modeled by $A_H H_a$. Free body diagram of the fluid body. (b) Free body diagram of the basic SDOF-system with acting interaction forces (and moment) from the TLCD dynamics. Seismic excitation indicated. Soil-structure interaction neglected.

2.1. Free Body Diagram of the Fluid in the TLCD

The *TLCD* is considered separated from the floor of the main structure, under combined in-plane horizontal w_t and vertical v_t floor excitations, see Figure (1a). After choosing the liquid mass m_t, the *TLCD* design parameters are the horizontal length of the liquid column B, the length of the liquid column in the

inclined pipe section at rest H, the horizontal and inclined cross-sectional areas A_B and A_H, respectively, and the opening angle of the inclined pipe section, $\pi/5 \le \beta \le \pi/2$. The relative and incompressible flow of the liquid inside the pipe is described by the liquid surface displacement, $u_1 = u_2 = u(t)$. If the piping system is sealed, the air inside the air chamber is quasi-statically compressed by the liquid surface in slow motion. Hence, the pressure difference, $\Delta p = p_2 - p_1$, when properly linearized, influences the undamped circular natural frequency of the *TLCD*, defined in Eq. (3). Applying the modified Bernoulli equation along the relative non-stationary streamline in the moving frame and in an instant configuration, Ziegler [8], yields the nonlinear parametrically excited equation of motion of the *TLCD*, Reiterer [6],

$$\ddot{u} + \delta_L |\dot{u}|\dot{u} + \omega_A^2 \left[1 + \frac{2\ddot{v}_t}{\omega_A^2 L_{eff}} sin\beta \right] u = -\kappa \ddot{w}_t, \tag{1}$$

where an averaged turbulent damping term, - experimentally verified, - has been added. The head loss coefficient δ_L can be increased by properly selecting a built-in orifice plate. In case of stationary flow, δ_L is tabulated for relevant pipe elements and cross-sections, e.g., sampled, in Ref. [10]. The geometry factor κ and the effective length L_{eff} of the liquid column, apparent in Eq. (1), are defined by

$$\kappa = \frac{B + 2H cos\beta}{L_{eff}}, \quad L_{eff} = 2H + \frac{A_H}{A_B}B, \tag{2}$$

see Ref. [5] for detailed derivations. The undamped circular natural frequency ω_A of the sealed *TLCD* includes approximately the air-spring effect where the pressure difference $\Delta p = p_2 - p_1$ is linearized with respect to the equilibrium pressure p_0, -an additional important design parameter, - by considering the first term of its Taylor series expansion. Assuming a polytropic state change, $D p(u) \approx 2n p_0 u / H_a, 1 \le n \le 1.4$, results. Consequently, the maximum stroke of air compression is limited to $|u| < 0.3 H_a$ to assure a good approximation of the eigenfrequency, for details see again either Ref. [5] or [6],

$$\omega_A = \sqrt{\frac{2g}{L_{eff}} \left(sin\beta + \frac{np_0/\rho g}{H_a} \right)} \tag{3}$$

In Eq. (3), p_0, ρ, g and H_a denote the initial (equilibrium) pressure in the air chamber, the liquid density, e.g. for water $\rho = 1000 kg/m^3$, the gravity constant $g = 9.81 m/s^2$, and the air spring height,

respectively. To avoid problems at the fluid-gas interface related to high speed limits the equilibrium pressure p_0 to about five times the atmospheric pressure. Consequently, also H_a is an important design variable, defining the volume of the air chamber in terms of the cross-sectional area A_H, see again Eq. (3). The limit $H_a \to \infty$ refers to $\Delta p = 0$ and thus applies approximately for *TLCD* with free flow of air between the air chambers, see again Figure (1a).

The time variant stiffness parameter in Eq. (1) contributes parametric excitation caused by the vertical floor acceleration $\ddot{v}_t$. Consequently, under special conditions of lightly damped *TLCD*, the instability phenomenon of parametric resonance is observed. A detailed study of this phenomenon and a sufficient condition to prevent parametric resonance and its possibly worsening effect on the damping behavior of the attached *TLCD* is presented in section 2.3.

In the course of the absorber optimization procedure, the turbulent damping in Eq. (1) has to be transformed into its equivalent linear one, $2\zeta_A \omega_A \dot{u}$. Demanding equally dissipated energy during one cycle (over a vibration period T and without any vertical excitation) for the nonlinear and the linear *TLCD* yields the relation

$$\int_0^T \left| \left(\delta_L \, |\dot{u}| \dot{u} + \omega_A^2 u \right) \dot{u} \right| dt = \int_0^T \left| \left(2\zeta_A \omega_A \dot{u} + \omega_A^2 u \right) \dot{u} \right| dt, \quad (4)$$

and, when substituting a time harmonic function, $u(t) = U_0 \cos \boldsymbol{w}_A t$, renders the equivalent viscous damping coefficient proportional to the amplitude,

$$\zeta_A = \frac{4U_0 \delta_L}{3\pi} \quad (5)$$

Under these conditions, Eq. (1) takes on its linearized form,

$$\ddot{u} + 2\zeta_A \omega_A \dot{u} + \omega_A^2 \left[1 + \frac{2\ddot{v}_t}{\omega_A^2 L_{eff}} \sin\beta \right] u = -\kappa \ddot{w}_t,$$

$$|u| \le U_0 \approx U_{max}, \quad (6)$$

The value of U_0, to be substituted in Eq. (5) in general forced vibrations, is determined by means of numerical simulations of the linear coupled *SDOF-TLCD* system, without vertical excitation, and commonly chosen as $U_0 = U_{max}$.

Considering the conservation of momentum of the fluid body, Figure (1a), determines the resultant interaction forces. The components, acting on the fluid body, relevant in the horizontal x', and, not to

be considered further, in the vertical z' directions, become

$$F_{x'} = m_f (\ddot{w}_t + \overline{\kappa}\ddot{u}), \quad \overline{\kappa} = \frac{B + 2H\cos\beta}{L_1}, \quad m_f = \rho A_H L_1$$

$$F_{z'} = m_f \left(\ddot{v}_t + \overline{\kappa}_1 \frac{1}{H} (u\ddot{u} + \dot{u}^2) \right), \quad \overline{\kappa}_1 = \frac{B + 2H\sin\beta}{L_1},$$

$$L_1 = 2H + \frac{A_B}{A_H} B, \quad (7)$$

where $\overline{\kappa}$ and $\overline{\kappa}_1$ are geometry factors and L_1 is a length, which becomes equal to L_{eff} for constant cross sectional area. Conservation of angular momentum with respect to the accelerated point of reference A, see again Figure (1a), yields the dynamic part of the undesired moment M_A acting on the fluid body, the static moment is $M_{A,stat} = m_f g \overline{\kappa} u$. Both moments and the force $F_{z'}$ are commonly neglected in the structural analysis.

2.2. Substructure Synthesis

The main system with assigned interaction forces from the *TLCD* dynamics is considered next, see Figure (1b), with horizontal $\ddot{w}_g$, and vertical $\ddot{v}_g$, ground accelerations prescribed. The external force resulting from wind gusts is not within the scope of this paper. The deformation is given by the displacement w with any time variant *P-Δ* effect neglected. The moving floor mass M includes the dead weight $m_D = m - m_f$ of the *TLCD* and modal masses of the columns. The field stiffness k, with geometric correction of prestressing by the dead weight taken into account for the CC-columns, see, e.g., Ref. [8] or Clough and Penzien [11], and light structural proportional damping r, are the remaining parameters.

Conservation of momentum of the floor mass M yields the relevant linear equation of motion of the main system

$$\ddot{w} + 2\zeta_S \boldsymbol{W}_S \dot{w} + \boldsymbol{W}_S^2 w = -\ddot{w}_g - \frac{1}{M} F_{x'},$$

$$\zeta_S = \frac{r}{2M \boldsymbol{W}_S}, \quad \boldsymbol{W}_S = \sqrt{k/M} \quad (8)$$

where $\boldsymbol{W}_S$ and $\boldsymbol{z}_S \ll 1$ denote the undamped circular natural frequency of the shear frame, and the linear viscous equivalent of its light structural damping, respectively. Inserting the coupling force $F_{x'}$ by substituting Eq. (7) into Eq. (8) renders, with Eq. (1) considered, the coupled system of equations of motion of the resulting two-*DOF*-system,

$$\ddot{w} + 2\zeta_S \, \mathbf{W}_S \, \dot{w} + \mathbf{W}_S^2 w = -\ddot{w}_g - \mu \ddot{w}_t - \mu \overline{\kappa} \ddot{u},$$

$$\ddot{u} + \delta_L |\dot{u}| \dot{u} + \omega_A^2 \left[1 + \frac{2\ddot{v}_t}{\omega_A^2 L_{eff}} \sin\beta \right] u = -\kappa \ddot{w}_t, \qquad (9)$$

$$w_t = w_g + w, \qquad v_t \approx v_g.$$

The mass ratio of fluid mass to the mass of the main system is denoted

$$\mu = \frac{m_f}{M} < 1. \qquad (10)$$

In order to provide highest possible transfer of energy from the main system to the *TLCD*, the mass ratio μ as well as the coupling factors κ and $\overline{\kappa}$ should be maximized. However, from the practical point of view the mass ratio is limited to $\mu = 0.5$-3%. The factors κ and $\overline{\kappa}$ depend on the geometry of the absorber, given in Eqs. (2) and (7) and should be close to one. They turn out equal for constant cross section of the pipe.

In order to prepare for the equation of motion of an *MDOF*-main structure with several, differently tuned *TLCD* attached, Eq. (9) is rewritten in its linearized matrix form and, leaving out parametric excitation, becomes

$$\tilde{M}_S \begin{bmatrix} \ddot{w} \\ \ddot{u} \end{bmatrix} + \tilde{C}_S \begin{bmatrix} \dot{w} \\ \dot{u} \end{bmatrix} + \tilde{K}_S \begin{bmatrix} w \\ u \end{bmatrix} = -\begin{bmatrix} M + m_f \\ \kappa \end{bmatrix} \ddot{w}_g, \qquad (11)$$

$$\tilde{M}_S = \begin{bmatrix} M + m_f & \overline{\kappa} m_f \\ \kappa & 1 \end{bmatrix}, \tilde{C}_S = \begin{bmatrix} 2\zeta_S \, \mathbf{W}_S M & 0 \\ 0 & 2\zeta_A \omega_A \end{bmatrix},$$

$$\tilde{K}_S = \begin{bmatrix} k & 0 \\ 0 & \omega_A^2 \end{bmatrix}.$$

2.3. Parametric Forcing of the Fluid by the Vertical Excitation: Cut-Off Damping

Under special conditions and for lightly damped *TLCD*, the undesired instability phenomenon of parametric resonance is observed, see Reiterer and Hochrainer [12]. Considering the linearized Eq. (6), the task of this section is to work out a sufficient condition in the form of a minimum linear damping ratio ζ_A in order to prevent any worsening effects from the vertical excitation. In absence of any horizontal excitation $\ddot{w}_t$, and further neglecting the turbulent and/or any viscous damping term, Eq. (6) further simplifies to the time-variant undamped oscillator equation,

$$\ddot{u} + \omega_A^2 \left[1 + \frac{2\ddot{v}_t}{\omega_A^2 L_{eff}} \sin\beta \right] u = 0 \qquad (12)$$

Assigning a time-harmonic vertical excitation $v_t = v_{t0} \cos\omega_z t$, Eq. (12) becomes a special type of Hill´s differential equation, namely the Mathieu equation [13],

$$\ddot{u} + \omega_A^2 \left[1 + \omega_z^2 \frac{2 v_{t0} \sin\beta}{\omega_A^2 L_{eff}} \cos\omega_z t \right] u = 0. \qquad (13)$$

Classically, Mathieu equation is the equation of motion of a plane pendulum with vertically moving point of suspension, see, e.g., Ziegler [8], which applies also to the conventional pendulum type of *TMD*, e.g. discussed by Soong and Dargush [1]. Dynamic stability of its solution has extensively been studied in the last century, for a recent review see Nayfeh and Mook [13]. The standard form of Eq. (13) requires substitution of the non-dimensional time $\tau = \omega_z t$, and, with its appropriate transformation results in

$$u'' + [\lambda + \gamma \cos\tau] u = 0, \; u' = \frac{du}{d\tau}, \qquad (14)$$

where λ and γ are identified as the non-dimensional stability parameters

$$\lambda = \frac{\omega_A^2}{\omega_z^2}, \quad \gamma = -\frac{2 v_{t0}}{L_{eff}} \sin\beta. \qquad (15)$$

The domains of stability for the solution of the Mathieu equation are cast in the Ince-Strutt diagram, Figure (2), where the stable domains are shaded. Inspection of Figure (2) identifies the most critical frequency ratio at $\lambda = 1/4$, (the domain of instability at this value is quite large) and also that damping strongly influences the occurrence of parametric resonance: If linear viscous damping of the dynamic system is taken into account, the domains of stability increase in the Ince-Strutt map, as indicated by hyperbolic curves in Figure (2). Hence, with sufficient damping of the dynamic system understood, parametric resonance does not occur. Nayfeh and Mook [13] derived the cut-off value of linear damping to prevent parametric resonance even under the most critical conditions at $\lambda = 1/4$. The sufficient condition to safely avoid parametric resonance even in this most critical case becomes, finally expressed in terms of the maximum vertical floor and/or ground acceleration,
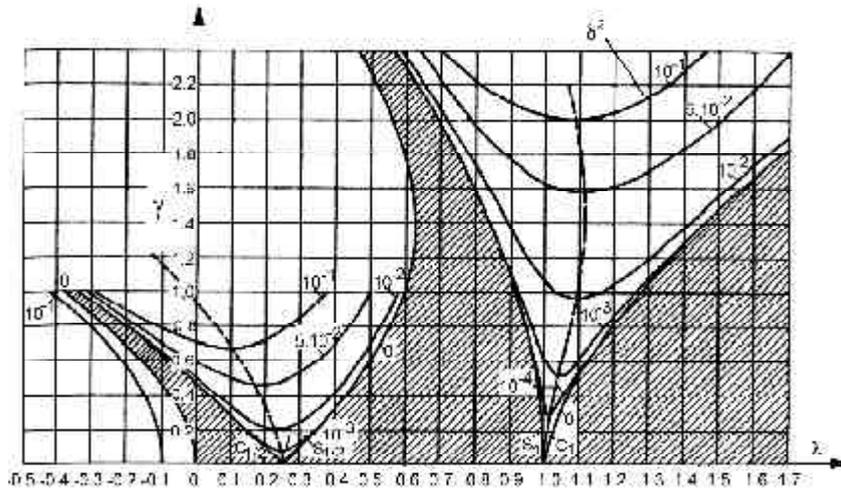
Figure 2. Parametric forcing of the linearized absorber model: domains of stability (shaded) and instability in the Ince-Strutt diagram, $\delta^2 = \lambda \zeta_A^2$, Klotter [14].

$$\zeta_A = \frac{4U_0\delta_L}{3\pi} > \frac{2v_{t0}}{L_{eff}}\sin\beta = \frac{max\left|\ddot{v}_g\right|}{4g\left(1+\dfrac{np_0/\rho g}{H_a\sin\beta}\right)} = \zeta_{A,0}. \quad (16)$$

Note the reduction of the cut-off value by the air spring effect in sealed *TLCD*. If the optimal linear damping coefficient of the *TLCD* is larger than the cut-off value $\zeta_{A,0}$, no worsening effect of its damping behavior of the horizontal vibrations occurs. The condition is subsequently confirmed experimentally and by numerical simulations. The vertical excitation can be safely neglected in Eq. (1) if the inequality (16) holds true.

3. Den Hartog (Modal) Tuning in Analogy to TMD: Horizontal Vibrations

For modal (*SDOF*) tuning of a classical *TMD*, the design parameters, denoted by a star, $\delta^* = \omega_A^*/W_S^*$ and ζ_A^* have to be suitably chosen. Classically Den Hartog [7], for time harmonic force excitation and undamped main system, $\zeta_S^* = 0$, derived these relations. Thus, in case of base acceleration, the non dimensional total acceleration of the floor mass, $1 + \ddot{w}/\ddot{w}_g$, is minimized by these *TMD* parameters, see, e.g., Ref. [1],

$$\delta_{opt}^* = \frac{1}{1+\mu^*}, \quad \zeta_{opt}^* = \sqrt{\frac{3\mu^*}{8(1+\mu^*)}}, \quad \mu^* = m^*/M^* \quad (17)$$

Slightly different parameters result for small mass ratios, when minimizing the relative floor acceleration, $\omega^2 w/\ddot{w}_g$,

$$\delta_{opt}^* = \frac{\sqrt{1-\mu^*/2}}{1+\mu^*}, \quad \zeta_{opt}^* = \sqrt{\frac{3\mu^*}{8(1+\mu^*)(1-\mu^*/2)}} \quad (18)$$

Hochrainer [5] compared the reduced Eq. (6) (putting $\ddot{v}_t = 0$) of the linearized *TLCD* with the equation of motion of a *TMD* and identified the following analogy by defining proper transformations. In Eqs. (17) and (18), the conjugate *TMD* mass ratio μ^* depends on the geometry factors κ and $\overline{\kappa}$, which are defined in Eqs. (2) and (7), respectively, and was identified in Ref. [5],

$$\mu^* = \frac{m^*}{M^*} = \frac{\kappa\overline{\kappa}\mu}{1+\mu(1-\kappa\overline{\kappa})}, \qquad \mu = \frac{m_f}{M}. \quad (19)$$

It is evident that every *TLCD* setup behaves like a *TMD* with absorber mass m^* attached to a moving floor mass M^*. The remaining mass $m_f - m^*$ has to be regarded as dead weight and thus, is added to the floor mass M^*. Thus, defining the equivalent *TMD* mass ratio μ_*, Eq. (19), renders the optimal values of the tuning parameters of the equivalent *TMD*-problem, δ^* and ζ_A^*. Subsequently, the inverse transformation to the *TLCD*-problem is applied, see again Hochrainer [5], rendering the optimal frequency ratio slightly modified and keeping the optimal linear damping ratio unchanged,

$$\delta = \frac{\omega_A}{W_S} = \frac{\delta^*}{\sqrt{1+\mu(1-\kappa\overline{\kappa})}}, \qquad \zeta_A = \zeta_A^*. \quad (20)$$

4. Bi-Axial, Time Harmonic and Transient Excitations of the Basic SDOF-System

The basic *SDOF*-system of Figure (1) is excited to steady state vibrations under the most critical forcing conditions and the influence of parametric excitation by the vertical motion is studied in a computer model and verified experimentally. Determination of the

cut-off value of damping of the *TLCD* is the main goal. Further, the turbulent damping of the fluid motion has to be verified. The basic *SDOF*-system with an optimized *TLCD* attached is exposed to the bi-axial transient forcing by the strong motion seismogram of the *N-S* Friuli 1976 earthquake, verifying the sufficient condition based on the cut-off damping.

4.1. Test Structure

A front view of the small scale testing facility in the Authors' laboratory is shown in Figure (3), consisting of a plane *SDOF*-pendulum with vertically moving suspension. The dynamic vertical forces are reduced since the dead weight is counter-balanced by a pulley mechanism. The lower rigid bar represents the floor of the main *SDOF*-structure. The open *TLCD* (free flow of air) consists of a Plexiglas pipe with rectangular cross section filled with colored water. Horizontal excitation is provided by an electromagnetic shaker of Brüel&Kjaer, Type 4808, connected to the lower rigid bar by a coil spring whose stiffness models the elastic columns of an equivalent *SDOF*-shear frame, shown in Figure (1b). The amplitude is limited to $w_{g0} \leq 0.004m$. A second actuator of the same type, forces the vertical motion with its stroke magnified by a simple lever construction to $v_{g0} = 0.016m$. Software LabView 7.0 provides the time-harmonic signals. Contact-less optical laser transducers, Type optoNCDT 1605, measure displacements as shown in Figure (3). The vertical acceleration is

recorded by the piezoelectric accelerometer of Brüel&Kjaer Type 4367. The latter is connected to a charge amplifier and an implemented integrator, to transform the measured accelerations into equivalent displacements. All measured signals are recorded by means of the software BEAM-DMCplusV3.7 through the board of Digital Amplifier System DMCplus (Hottinger Baldwin Messtechnik, *HBM*). A novel sensor, consisting of two pairs of wire electrodes whose resistance depends on the water level, measures the motion of the liquid surface, Reiterer and Hochrainer [15]. To compensate for several nonlinearities, the electrodes are in series connection. For further processing, the electronic signal is band-pass-filtered, in order to reduce the static drift and any high frequency noise. The measured signal is recorded again by the software BEAM-DMCplusV3.7, whereby the measured changes of resistance are transformed into the equivalent displacement of the liquid surface by means of a nonlinear transfer function, obtained by calibrating the fluid motion in the *TLCD*.

The parameters of *TLCD* and *SDOF* basic-system are selected according to the laboratory model. The ratio of fluid mass m_f to the moving floor mass of the main system M is chosen rather high, $\mu = m_f/M = 0.071$. Hence, with floor mass $M = 2.96kg$, the water mass is $m_f = 0.21kg$. The dimensions of the open *TLCD* in Figure (1a) are: $\beta = \pi/4$, $A_H = A_B = 0.0005m^2$, $\kappa = \bar{\kappa} = 0.84$, $L_{eff} = L_1 = 0.42m$ in Eq. (3), rendering $f_A = \omega_A/2\pi = 0.90Hz$. The *TLCD* is tuned to frequency, by adjusting the natural frequency of the *SDOF*-basic system which is simpler done in the laboratory. Selecting Eq. (18), Eq. (20) yields the optimal frequency ratio $\delta_{opt} = \omega_A/\Omega_{S,opt} = 0.94$ and hence, $f_{S,opt} = f_A/\delta_{opt} = 0.96Hz$. The optimal equivalent linear damping becomes $\zeta_{A,opt} = 0.11$.

Free vibration tests of main system and *TLCD* were performed to determine and verify the natural frequencies and damping coefficients. Damping is stepwise increased to the final optimal value. The lightest linearized viscous damping terms, $\zeta_A = 0.045$ and $\zeta_S = 0.01$, have been observed by inspection of the decay rates of free vibration in laboratory testing. ζ_A is the mean value of a number of free vibration tests within an amplitude range of $U_0 = 40\text{-}60mm$.

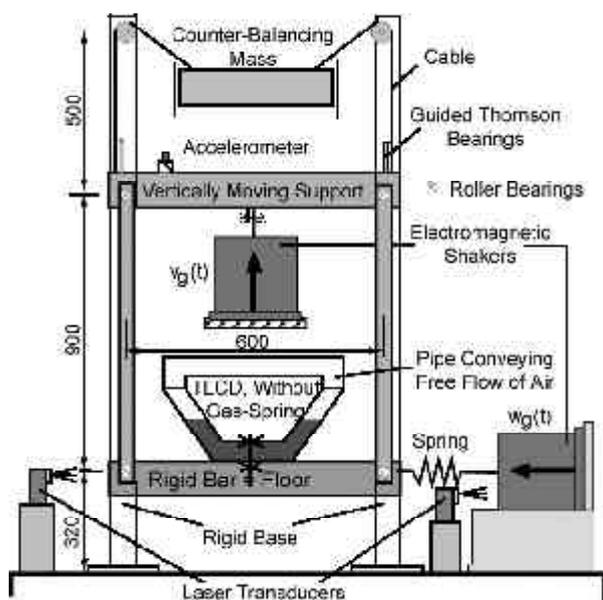The cut-off value of parametric resonance, defined in Eq. (16), relevant for the laboratory testing is

Figure 3. Front view of the experimental model set-up, equivalent to the basic SDOF-system.

$$\zeta_{A,0} = \frac{2v_{g0}}{L_{eff}} \sin\beta = 0.054 \begin{cases} < \zeta_{A,opt} = 0.11 \\ > \zeta_A = 0.045 \end{cases} \quad (21)$$

The results of the numerical simulations are compared with the experimental output in section 4.2.

4.2. Experimental and Numerical Results of Steady State Vibrations. TLCD Tuned to Frequency. Verification of Cut-Off and Turbulent Damping

The experimentally and numerically obtained results in a time window under time harmonic critical forcing are shown in Figures (4a) and (4b). The vertical forcing frequency $\omega_z = 2\omega_A$ (stability parameter $\lambda = 1/4$), and the amplitude $v_{g0} = 0.016m$ are kept constant within the range of simulations. The bold line represents the steady state vibration without any vertical excitation and the thin line indicates the influence of the assigned vertical excitation. It is important to emphasize that the chosen combination of the values $f_z = 1.80Hz$ and $v_{g0} = 16mm$ leads to parametric resonance for the light damping assigned, as predicted by Eq. (21). The beat phenomenon discussed in Ref. [16] can be seen in Figures (4a) and (4b) that shows an excellent agreement between experimental and predicted theoretical results, with averaged turbulent damping $\delta_L = 1.33$ considered. However, the solution of the linearized equation of motion with equivalent linear damping $\zeta_A = 0.045$ kept constant, grows beyond bounds. Thus, the linearized model turns out to be insufficient for numerical simulation, see Figure (4c), and note the different scale in Figure (4b). In order to obtain good agreement between numerical and experimental results, the simulated *TLCD* must be always considered with an averaged turbulent damping assigned. Consequently, the various linear viscous damping coefficients are transformed to their turbulent equivalent, by means of the relation given in Eq. (5), $\delta_L = 3\pi\zeta_A / 4 U_0$ where U_0 is determined by numerical simulations of the linearized coupled system without vertical excitation, considering the steady state vibration at a discrete horizontal forcing frequency ω_x, and subsequently by choosing $U_0 = U_{max}$. The Dynamic Magnification Factor (*DMF*) for the parametrically excited coupled main system/*TLCD* is determined at discrete values of the horizontal forcing frequency $f_{x,i}$. Thereby, the frequency dependent turbulent damping term $\delta_{L,i}$ has to be varied over the frequency range of interest. In order to determine the appropriate values defined in Eq. (5), $U_{0,i}$ must be specified as the maximum value of the vibration amplitude, i.e., $U_{0,i} = U_{max,i}$ calculated in the linearized model without vertical excitation under steady state conditions. DMF_i at the forcing
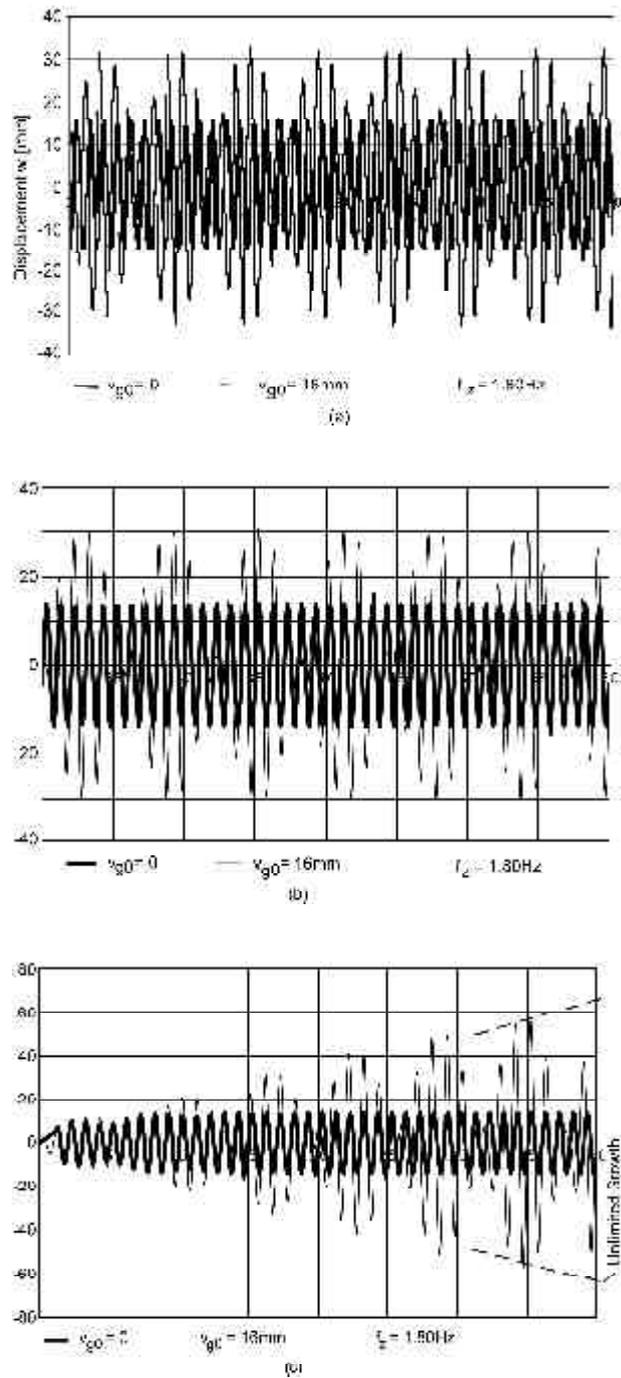
Figure 4. Steady state response of the basic SDOF-system. Horizontal and vertical forcing frequencies, $f_x = 1.00$ Hz and $f_z = 1.80Hz$. TLCD tuned to frequency. Light turbulent damping $\rightarrow \delta_L = 1.33$ constant. (a) Experimental results. (b) Numerical results, light turbulent damping (c) Numerical results for equivalently linear damped TLCD $\rightarrow \zeta_A = 0.045 =$ constant. Insufficient modeling.

frequency $f_{x,i}$ is defined by

$$DMF_i = \left| \frac{w_{max,i}}{w_{g0}} \right|, \tag{22}$$

where $w_{max,i}$ is defined by the steady state response of the nonlinear, parametrically excited coupled system.

An excellent agreement between experimental results and those derived by computational simulations is observed in Figure (5). For light damping, Figures (5a) and (5b) show that parametric resonance approximately doubles the resonant peaks. However, as predicted by Eq. (21) for the optimally damped *TLCD*, no influence of parametric resonance is observed for the range of vertical excitation amplitudes considered, as shown in Figure (5c). Analogous to Den Hartog´s solution, the frequency response function exhibits two fixed-points at the same height and in addition, as an effect of the optimal damping of the *TLCD*, the tangents are horizontal indicating minimization of the extreme values. Hence, it can be concluded that parametric resonance only influences lightly damped *TLCD* and disappears in the case of optimal and sufficient damping, within the considered range of vertical excitation amplitudes. Prediction of Eq. (21) is verified.

4.3. Transient Bi-Axial Forcing of the Basic SDOF-System by the Friuli 1976 Seismogram. TLCD Optimally Tuned. Verification of Cut-Off Damping

The scaled European *N-S* Friuli 1976 earthquake (station name: Tolmezzo-Diga Ambiesta, Italy) downloaded from the Internet Site for European Strong Motion Data [17] is plotted in Figure (6). The duration of strong motion phase takes only a few seconds, from about $t = 3$ to $t = 8s$ and the main energy is supplied in the low frequency range, from about $f = 2$ to $f = 5Hz$. Since the natural frequencies of the tested system are $f_S = 0.96Hz$ and $f_A = 0.90Hz$, the time history of the considered quake is adjusted to the laboratory model. For further processing the given sampling rate $\Delta t = 0.01s$ is doubled which results in increasing the duration of the strong motion phase. The *N-S* Friuli seismogram is applied in both directions, horizontally as well as
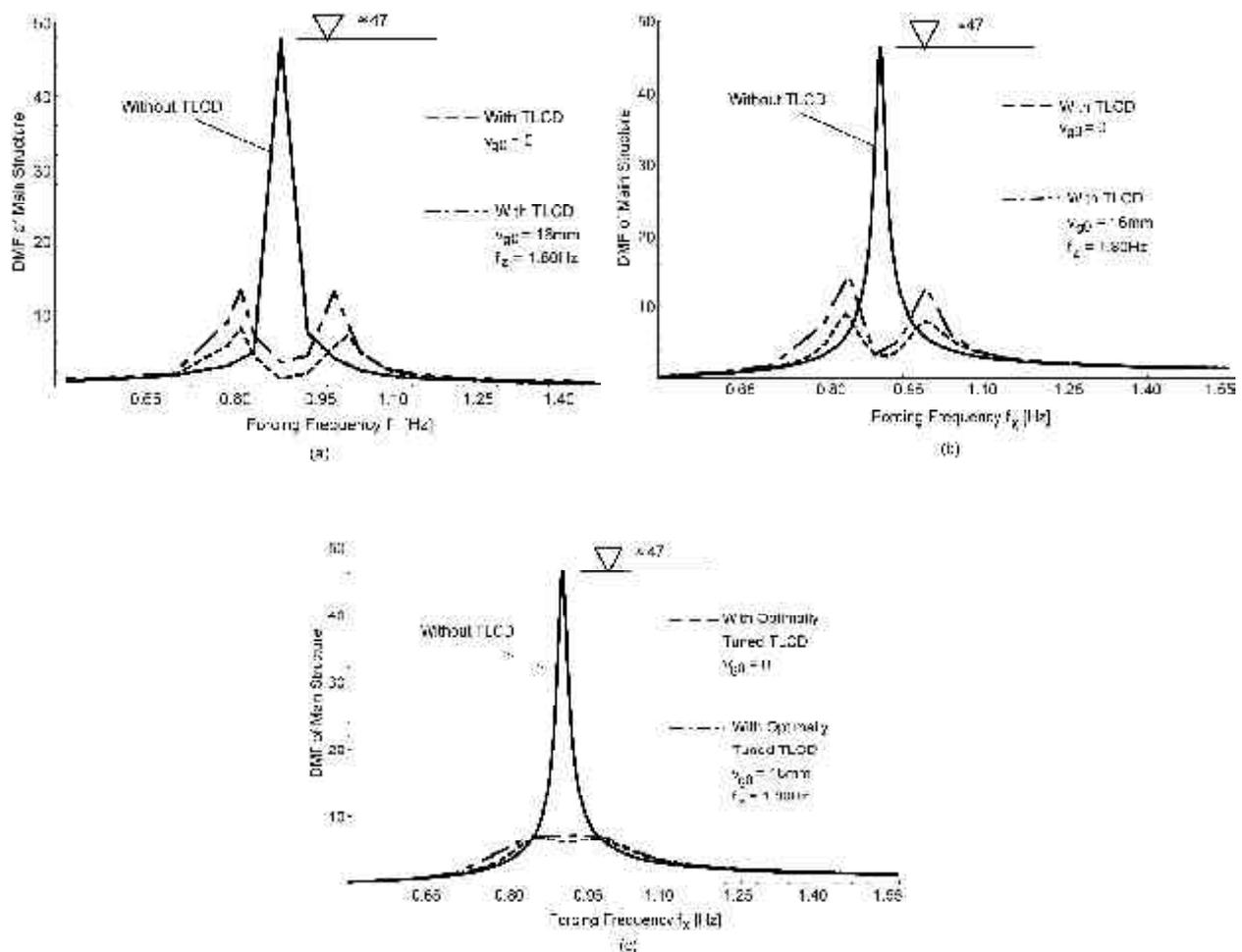
Figure 5. Dynamic magnification factor (DMF) of the basic SDOF- system, $\left| w_{max} / w_{g0} \right|$. Data likewise to Figure (4), f_x swept. (a) Experimental results. (b) Numerical simulation. TLCD tuned to frequency with light turbulent damping adjusted at discrete frequencies to the steady state amplitude, $\delta_{L,i} \rightarrow U_{0,i}$, ($\rightarrow \zeta_A = 0.045$ assigned). (c) Experimental and numerical results. Optimally tuned TLCD. In the simulations turbulent damping adjusted at discrete frequencies to the steady state amplitude, $\delta_{L,i} \rightarrow U_{0,i}$, ($\rightarrow \zeta_{A,opt} = 0.11$ assigned).
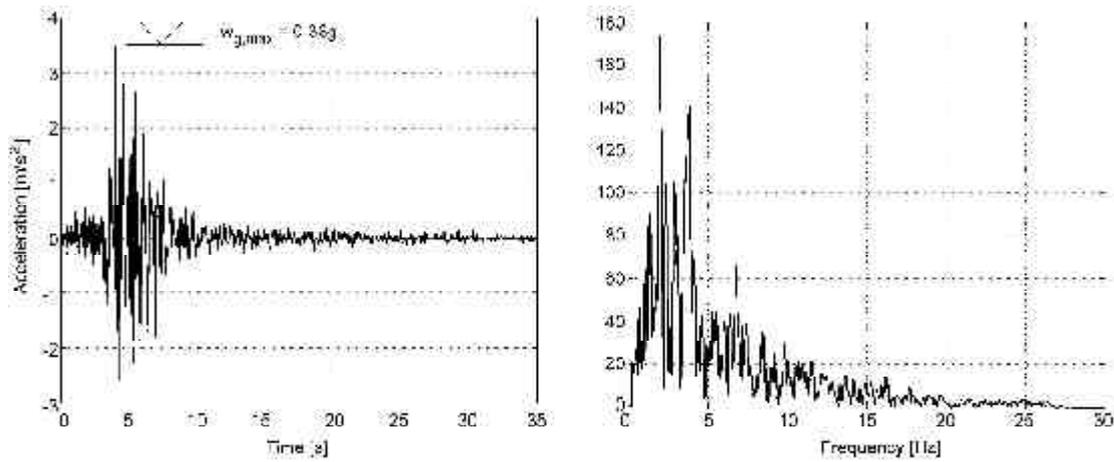
Figure 6. N-S Friuli 1976 earthquake (station name: Tolmezzo-Diga Ambiesta, Italy) in time and frequency domain. Source: EU-funded European Strong Motion Data [17].

vertically with one and the same strength. Again nonlinear turbulent damping is taken into account in the equation of motion of the *TLCD*, which ensures a stable motion even in case of light damping. Estimating $U_{max} = 80mm$ yields together with $\zeta_{A,opt} = 0.11$ the nonlinear optimal turbulent damping coefficient, Eq. (5), $\delta_L = 3.24$.

Furthermore, the sufficient condition to prevent the influence of vertical excitation has to be checked, Eq. (16) with $H_a \rightarrow \infty$,

$$\zeta_{A,0} = \frac{max|\ddot{v}_g|}{4g} = 0.09 < \zeta_{A,opt} = 0.11, \tag{23}$$

where the maximum vertical base acceleration is given by $\ddot{w}_{g,max} = \ddot{v}_{g,max} = 0.36g$, see again Figure (6). Thus, the optimal linearized damping ratio $\zeta_{A,opt}$ exceeds the cut-off value $\zeta_{A,0}$ and no worsening effect of parametric resonance is expected.

Simulations of the nonlinear, parametrically excited system are performed using Simulink's time integration tool, which is smoothly integrated into the *MATLAB* scientific computing environment. Figure (7a) illustrates the time history response of the main structure with and without *TLCD* in nonlinear modeling attached, under combined horizontal and vertical seismic excitations.

In Figure (7b), the time history responses of the coupled system with and without vertical seismic activation taken into account are shown. Both lines
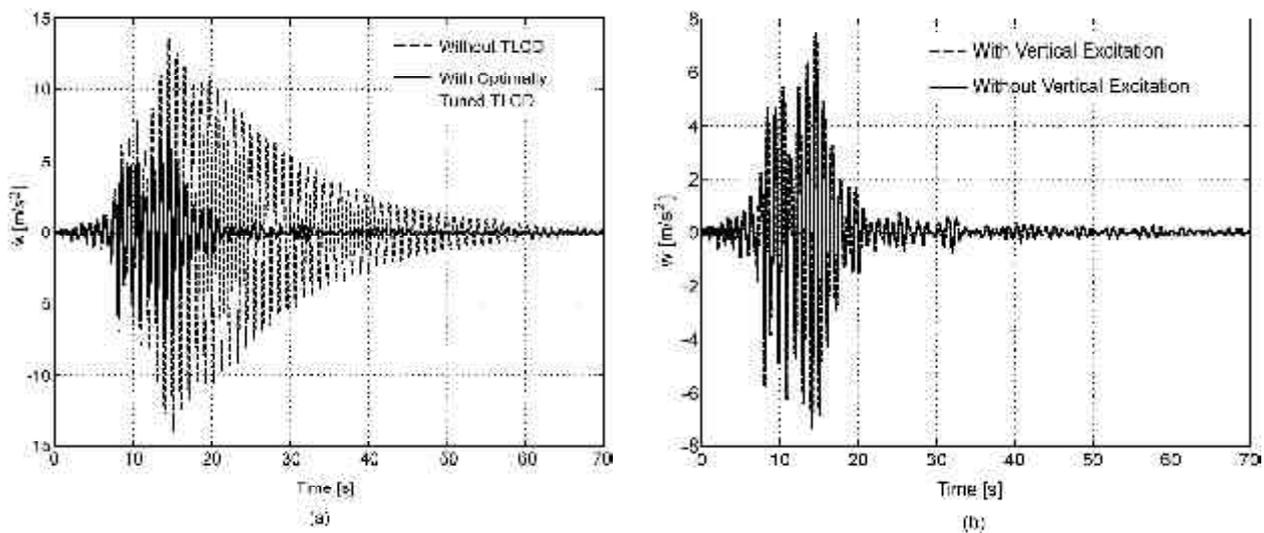
Figure 7. Relative acceleration of the floor mass of the basic SDOF-system forced by the N-S Friuli 1976 earthquake. (a) Bi-axial excitations, identical seismograms applied. Optimally tuned TLCD (turbulent damping $\rightarrow \delta_L = 3.24$ = constant). Note the 50% reduction of maximum peak. (b) Responses under bi-axial excitations (note the different scale in Figure (7a) and under uni-axial horizontal excitation. Cut-off damping verified by inspection.

nearly coincide and thus confirm, that due to the vertical base excitation no undesired influence on the optimal damping behavior of the *TLCD* is observable.

5. State Space Optimization of Multiple TLCD Attached to MDOF-Systems

In case of multiple *TLCD* attached to *MDOF*-systems the tuning process is best performed in two steps. At first, the linearized computer model is tuned with respect to a selected mode of the main system using the *TLCD-TMD* analogy, as presented in section 3. Subsequent improvements of the performance in *MDOF*-systems are achieved by considering the neighboring modes as well in a state space representation, by minimizing the weighted squared area of the frequency response function (*FRF*). Hence, the coupled equations of motion have to be transformed to the state space. The *N-DOF* main system with a number of $n \ll N$ *TLCD* installed at proper locations, is described by the set of matrix equations, in a hyper matrix formulation,

$$\tilde{M}_S \begin{bmatrix} \ddot{\bar{w}} \\ \ddot{\bar{u}} \end{bmatrix} + \begin{bmatrix} \tilde{C} & \tilde{0} \\ \tilde{0} & \tilde{C}_f \end{bmatrix} \begin{bmatrix} \dot{\bar{w}} \\ \dot{\bar{u}} \end{bmatrix} + \begin{bmatrix} \tilde{K} & \tilde{0} \\ \tilde{0} & \tilde{K}_f \end{bmatrix} \begin{bmatrix} \bar{w} \\ \bar{u} \end{bmatrix}$$

$$= -\begin{bmatrix} \tilde{M}\bar{r}_S + \tilde{L}\tilde{M}_f \bar{i} \\ \tilde{\kappa} \bar{i} \end{bmatrix} \ddot{w}_g, \tag{24}$$

set up in extending Eq. (11). The sparse position matrix with dimension $N \times n$,

$$\tilde{L} = \begin{bmatrix} 1 & 0 & 1 \\ \vdots & \vdots & \vdots \\ 0 & 1 & 0 \\ \vdots & \vdots & \vdots \\ 0 & 0 & 0 \end{bmatrix} \leftarrow DOF \text{ to be influenced} \tag{25}$$

$$\uparrow$$
number of *TLCD*

apparent in Eq. (24), enters the generalized mass matrix as well,

$$\tilde{M}_S = \begin{bmatrix} \tilde{M} + \tilde{L}\tilde{M}_f \tilde{L}^T & \tilde{L}\tilde{M}_f \tilde{\bar{\kappa}} \\ \tilde{\kappa}\tilde{L} & \tilde{I} \end{bmatrix}. \tag{26}$$

$\tilde{M}, \tilde{C}$ and $\tilde{K}$ are mass, damping and stiffness matrix of the main system and the following diagonal matrices are self explanatory,

$$\tilde{M}_f = diag[m_{f1},..., m_{fn}],$$

$$\tilde{C}_f = diag[2\zeta_{A1}\omega_{A1},..., 2\zeta_{An}\omega_{An}],$$

$$\tilde{K}_f = diag[\omega_{A1}^2,..., \omega_{An}^2],$$

$$\tilde{\kappa} = diag[\kappa_1,..., \kappa_n],$$

$$\tilde{\bar{\kappa}} = diag[\bar{\kappa}_1,..., \bar{\kappa}_n]. \tag{27}$$

together with the static influence vector $\tilde{r}_S$, which, for the single point base excitation is $\bar{r}_S = \bar{i} = [1 \ 1 \ 1 \ ... \ 1]^T$.

Eq. (24) is easily converted to a first order state space representation by introducing the new state vector $\bar{z} = [\bar{w} \bar{u} \ \dot{\bar{w}} \dot{\bar{u}}]^T$, and its time derivative

$$\dot{\bar{z}} = (\tilde{A} + \tilde{B}\tilde{R})\bar{z} - \bar{e}_g \ddot{w}_g,$$

$$\bar{e}_g = \begin{bmatrix} \bar{0} & \bar{0} & \tilde{M}_S^{-1} \begin{pmatrix} \tilde{M}\bar{r}_S + \tilde{L}\tilde{M}_f \bar{i} \\ \tilde{\kappa}\bar{i} \end{pmatrix} \end{bmatrix}^T, \tag{28}$$

to render the standard form of control theory. The system matrix $\tilde{A} + \tilde{B}\tilde{R}$, apparent in Eq. (28), should be kept separated since, at this stage, only the elements of $\tilde{A}$ and $\tilde{B}$,

$$\tilde{A} = \begin{bmatrix} \tilde{0} & \tilde{0} & \tilde{I} & \tilde{0} \\ \tilde{0} & \tilde{0} & \tilde{0} & \tilde{I} \\ -\tilde{M}_S^{-1}\begin{pmatrix} \tilde{K} & \tilde{0} \\ \tilde{0} & \tilde{0} \end{pmatrix} & -\tilde{M}_S^{-1}\begin{pmatrix} \tilde{C} & \tilde{0} \\ \tilde{0} & \tilde{0} \end{pmatrix} \end{bmatrix},$$

$$\tilde{B} = \begin{bmatrix} \tilde{0} & \tilde{0} & \tilde{I} & \tilde{0} \\ \tilde{0} & \tilde{0} & \tilde{0} & \tilde{I} \\ -\tilde{M}_S^{-1}\begin{pmatrix} \tilde{I} & \tilde{0} \\ \tilde{0} & \tilde{I} \end{pmatrix} & -\tilde{M}_S^{-1}\begin{pmatrix} \tilde{I} & \tilde{0} \\ \tilde{0} & \tilde{I} \end{pmatrix} \end{bmatrix} \tag{29}$$

are known, whereas $\tilde{R}$ contains the unknown linear *TLCD* design parameters,

$$\tilde{R} = \begin{bmatrix} \tilde{0} & \tilde{0} & \tilde{0} & \tilde{0} \\ \tilde{0} & \tilde{K}_f & \tilde{0} & \tilde{0} \\ \tilde{0} & \tilde{0} & \tilde{0} & \tilde{0} \\ \tilde{0} & \tilde{0} & \tilde{0} & \tilde{C}_f \end{bmatrix}. \tag{30}$$

The steady-state solution in frequency space is

$$\bar{z}(\omega) = [i\omega\tilde{I} - (A + \tilde{B}\tilde{R})]^{-1}\bar{e}_g. \tag{31}$$

In order to find the optimal tuning parameters of *TLCD* it is common practice to minimize a suitable performance index, e.g., defined by the infinite integral of the weighted sum of quadratic state variables of the main system $\bar{z}_S$, in the frequency domain, see e.g. Müller and Schiehlen [15],

$$J = \int_{-\infty}^{\infty} \vec{z}_S^T(\omega)\tilde{S}\,\vec{z}_S(\omega)d\omega = 2\pi\vec{e}_g^T\tilde{P}\vec{e}_g \to min, \qquad (32)$$

where $\tilde{P}$ is the solution of the algebraic Lyapunov matrix equation,

$$\left(\tilde{A} + \tilde{B}\tilde{R}\right)^T \tilde{P} + \tilde{P}\left(\tilde{A} + \tilde{B}\tilde{R}\right) = -\tilde{S}. \qquad (33)$$

$\tilde{S}$ is a symmetric, positive semi-definite weighing matrix, which offers the possibility to emphasize the importance of selected components of the state space vector. The matrix solution $\tilde{P}$ of Eq. (33) is numerically evaluated by means of the software *MATLAB*. The minimum search in the Eq. (32) is best performed by the *MATLAB* optimization toolbox, "*fminsearch*", when substituting Den Hartog´s modal tuning parameters, as discussed in section 3, as start values. The modal analysis of the main system with separated eigenfrequencies understood, is classical and not further discussed here.
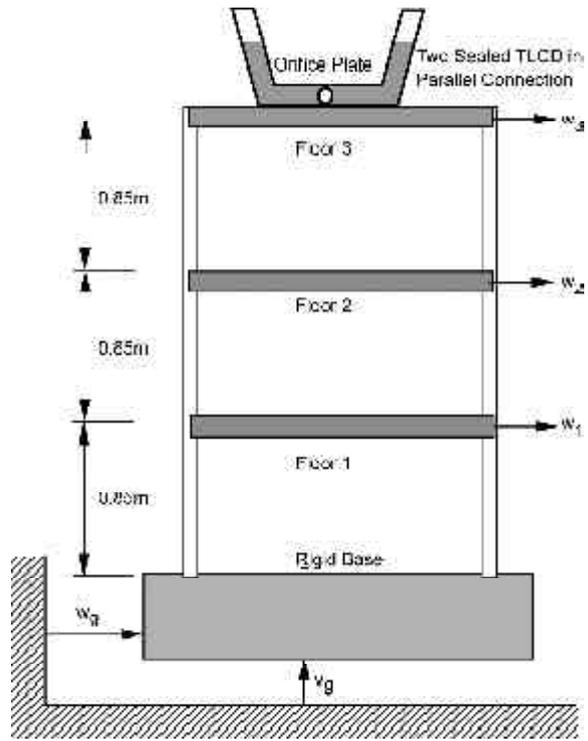
6. A Three-DOF-Benchmark Structure under Combined Earthquake Loadings

The effectiveness of passive *TLCD* in vibration reduction is demonstrated for a plane three-*DOF*-benchmark test structure under earthquake loading, which has also been studied by Hochrainer [5] taking into account the horizontal seismic activation only. Subsequently the vertical excitation is considered and the *TLCD* is split into two *TLCD* in parallel connection. Based on a benchmark definition paper, see Spencer et al [9], a scale model of the original structure was built at the National Center of Earthquake Engineering (*NCEER*) at Buffalo, *N.Y.*, which requires the mass reduction by 1:16 with respect to the original structure, time shortened by 1:2 and the displacement scale of 1:4, the acceleration thus, remains unchanged. In the current numerical study the structural model with a total mass of 2943*kg* is equipped with two, sealed passive *TLCD* in parallel connection on the 3rd top floor, as illustrated in Figure (8). Splitting a single passive *TLCD* in two *TLCD* in parallel connection requires fine-tuning in the state space. Modal (*SDOF*) tuning as discussed above is performed in a first step.

Hochrainer [5], provided the ortho-normalized eigenvectors and the well-separated undamped natural frequencies,

$$\vec{\phi}_1 = \begin{pmatrix} 0.2015 \\ 0.5472 \\ 0.8123 \end{pmatrix}, \vec{\phi}_2 = \begin{pmatrix} 0.6782 \\ 0.5204 \\ -0.5189 \end{pmatrix}, \vec{\phi}_3 = \begin{pmatrix} -0.7067 \\ 0.6555 \\ -0.2662 \end{pmatrix},$$
$$ (34)$$
$$f_{S1} = 2.38\,Hz, \qquad f_{S2} = 7.44\,Hz, \qquad f_{S3} = 12.29\,Hz,$$

Figure 8. Scaled three-DOF-benchmark test structure under combined horizontal and vertical earthquake loads, with two, sealed passive TLCD in parallel connection on the top floor.

of the main test system. The light modal damping ratios are set to $\zeta_{S1} = 1\%$, $\zeta_{S2} = 2\%$ and $\zeta_{S3} = 3\%$, respectively. The attached, necessarily sealed *TLCD* will be tuned with respect to the fundamental natural frequency of the model choosing the mass ratio 2% with respect to the modal mass of the fundamental mode, $M_1^* = 1531\,kg$. Thus, the total fluid mass is $m_f = 30\,kg$.

6.1. Optimal Design of Two, Sealed TLCD, Tuned to the Basic Mode

Subsequently, the total fluid mass is split in two *TLCD* in parallel connection, $m_{f1} = m_{f2} = 15\,kg$. The following design parameters are chosen, see Figure (1a): horizontal and inclined lengths of the liquid column, $B = 1.5\,m$ and $H = 0.5\,m$, constant cross-sectional areas $A_H = A_B = 0.012\,m^2$, angle of the inclined pipe section $\beta = 40°$. Hence, the effective length of the liquid column and the geometry factors, determined in Eqs. (2) and (7), become $L_{eff} = L_1 = B + 2H = 2.5\,m$ and $\kappa = \bar{\kappa} = 0.91$.

In a first step, the optimal absorber frequencies ω_{Ai} and the linearized viscous damping ζ_{Ai}, i = 1, 2 are determined using the *TLCD-TMD* analogy and considering the fundamental modal coordinate to be optimized. Eq. (19) yields $\mu_1^* = \mu_2^* = 0.0081$ to be

substituted in Eq. (17). Evaluating Eq. (20) renders identical optimal design parameters of both *TLCD*: $f_{A1} = f_{A2} = 2.36Hz$, $\zeta_{A1} = \zeta_{A2} = 0.055$. Improvements of their performance are achieved by minimizing the frequency domain based quadratic performance index in the state space representation. The state vector of the main system, $\bar{z}_S = [w_1, w_2, w_3, \dot{w}_1, \dot{w}_2, \dot{w}_3]^T$, to be substituted in Eq. (32), contains the TLCD quantities, e.g., the liquid surface displacement and velocity not explicitly. However, the damping effect of the modally tuned *TLCD* is hidden in the system's dynamics, Eq. (31), and thus in the structural response vector $\bar{z}_S$. The relevant matrices, $\tilde{A}, \tilde{B}$ and $\tilde{R}$, Eqs. (29) and (30), for the plane frame with *TLCD* on top, Figure (8), have standard form, explicitly derived in Ref. [5], and are not repeated here. Having chosen the weighing matrix, $\tilde{S} = diag[1 0 1 0 1 0 1 1]$, the numerical minimization of the performance index is started with Den Hartog´s modal tuning parameters. Calling "*fminsearch*" within the *MATLAB* optimization toolbox renders the new optimal tuning parameters significantly changed: $f_{A1} = 2.25Hz$, $\zeta_{A1} = 0.039$, $f_{A2} = 2.46Hz$, $\zeta_{A2} = 0.042$. It is noticed that f_{A1} is smaller and f_{A2} is larger than the fundamental natural frequency $f_{S1} = 2.38Hz$ to be influenced by the *TLCD*. This fact increases the robustness of the attached damping device in view of expected changes of model parameters (mass, stiffness) during the operating life. The maximum gain through the action of the two optimally tuned passive *TLCD* in parallel connection at the fundamental frequency of the main structure is indicated with about $30dB$ in Figure (9).
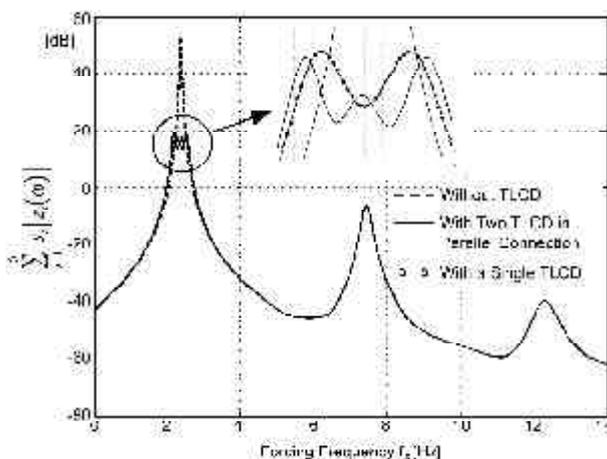
Figure 9. Frequency response functions, FRF, of the sum of weighted absolute state space variables of the three-DOF-test structure. Uni-axial, horizontal time harmonic forcing. Damping of the two, optimally tuned TLCD is considered equivalently linear viscous and independent of the forcing frequency. Damping characteristic zoomed and compared to a single TLCD action.

In order to realize the optimal natural frequencies of the *TLCD* in practice, the air spring effect can be activated. Eq. (3) is solved for the height H_a,

$$H_a = \frac{2 n p_0}{\rho \omega_A^2 DL_{eff}}, \quad DL_{eff} = L_{eff} - \frac{2 g \sin\beta}{\omega_A^2}, \qquad (35)$$

where ΔL_{eff} defines the difference of the effective lengths of the liquid column with and without the air-spring effect taken into account. Subsequently, assuming the polytropic index $n = 1.2$ and assigning just the initial atmospheric pressure in equilibrium to each *TLCD*, $p_0 = 10^5 Pa$, the air chamber heights, $H_{a1} = 0.49m$ and $H_{a2} = 0.41m$ result.

6.2. Combined Earthquake Loadings by the N-S Friuli 1976 and the El Centro Seismograms. Verification of Cut-Off Damping

Since the system under consideration is still a scaled model, the time scale of the acceleration input is increased by a factor of two, i.e., the simulated strong motion occurs in half of the recorded time. The *N-S* Friuli 1976 earthquake, defined in Figure (6) is considered properly scaled next. The corresponding cut-off values of the linearized damping coefficients for the sealed *TLCD* are determined by Eq. (16),

$$\zeta_{A,0,1} = \frac{max|\ddot{v}_g|}{4g\left(1 + \frac{np_0/\rho g}{H_{L1}\sin\beta}\right)} = 0.0023 < \zeta_{A1} = 0.039,$$

$$\zeta_{A,0,2} = \frac{max|\ddot{v}_g|}{4g\left(1 + \frac{np_0/\rho g}{H_{L2}\sin\beta}\right)} = 0.0019 < \zeta_{A2} = 0.042, \qquad (36)$$
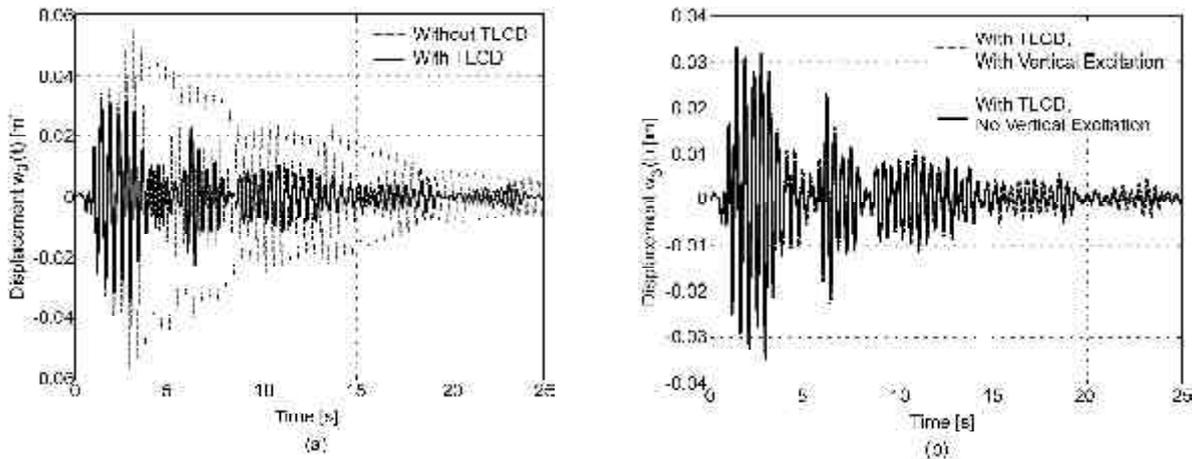
and, consequently, no worsening effects on the optimal damping behavior of the sealed *TLCD* are expected. The numerical simulations are performed using *MATLAB*/Simulink, considering the *TLCD* with turbulent damping, Eq. (1) holds true. The averaged optimal turbulent damping terms, determined by Eq. (5), are $\delta_{L1} = 0.61$ and $\delta_{L2} = 0.65$, assigning the maximum vibration amplitudes (forecast by uni-axially exciting the linear model) $U_{max,1} = U_{max,2} = 0.15m$. The results for the horizontal top floor displacement w_3, with and without two *TLCD* with turbulent damping, under combined and assigned horizontal and vertical seismic activation by the *N-S* Friuli quake are illustrated in Figure (10a). A large reduction of the maximum vibration amplitude is observed, thus the passive action of the *TLCD* seems to be well suited to

counteract the combined earthquake loadings. Nevertheless, a transient vibration peak remains nearly unaffected during the early part of the strong motion phase, see again Figure (10a). A significant reduction of these early transient peaks requires active control of the air spring, by proper external pressure supply from a pressurized gas-reservoir, rendering the active *TLCD* (*ATLCD*). Hochrainer [5] performed detailed investigations of *ATLCD*. The top floor displacements are illustrated in Figure (10b) with and without vertical seismic activation taken into account. The time records indicate no visible influence of the vertical earthquake loading verifying the condition based on the cut-off damping, Eq. (36). The seismogram of the *N-S* El Centro earthquake with a peak ground acceleration of $\ddot{w}_{g,max} = 0.35g$ is applied alternatively, again in both, horizontal and vertical directions, with the same

strengths, illustrated in Figure (11). Since the system under consideration is still the scaled model, the time scale of the acceleration input is increased by the factor of two. The numerical simulations are analogously performed using *MATLAB*/Simulink and considering the *TLCD* with turbulent damping. Since the sufficient condition, Eq. (16), is again verified, no worsening effect of the vertical excitation is expected,

$$\zeta_{A,0,1} = \frac{max\left|\ddot{v}_g\right|}{4g\left(1+\frac{np_0/\rho g}{H_{L1}sin\beta}\right)} = 0.0022 < \zeta_{A1} = 0.039,$$

$$\zeta_{A,0,2} = \frac{max\left|\ddot{v}_g\right|}{4g\left(1+\frac{np_0/\rho g}{H_{L2}sin\beta}\right)} = 0.0019 < \zeta_{A2} = 0.042. \tag{37}$$
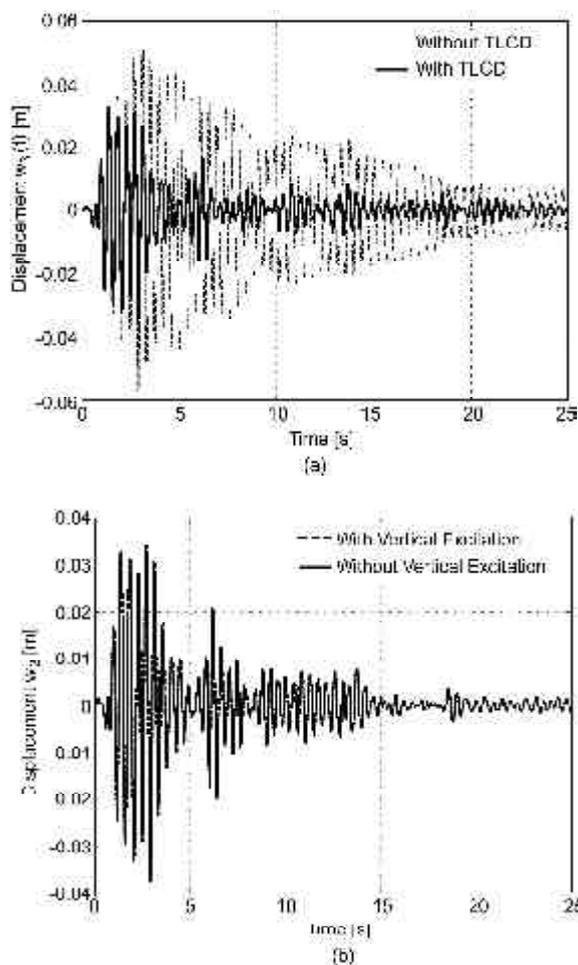

Figure 10. Top floor displacements of the scaled three-DOF-test structure forced by the scaled N-S Friuli seismogram. (a) Bi-axial excitations, identical seismograms applied. Two optimally tuned TLCD in parallel connection (turbulent damping $\rightarrow \delta_{L1} =$ 0.61= constant, $\rightarrow \delta_{L2} = 0.65$= constant). Note the possibly insufficient reduction of the maximum peak in the transient regime by $\approx$20%. (b) Responses under bi-axial excitations (note the different scale in Figure (10a)) and under uni-axial horizontal excitation. Cut-off damping verified by inspection.
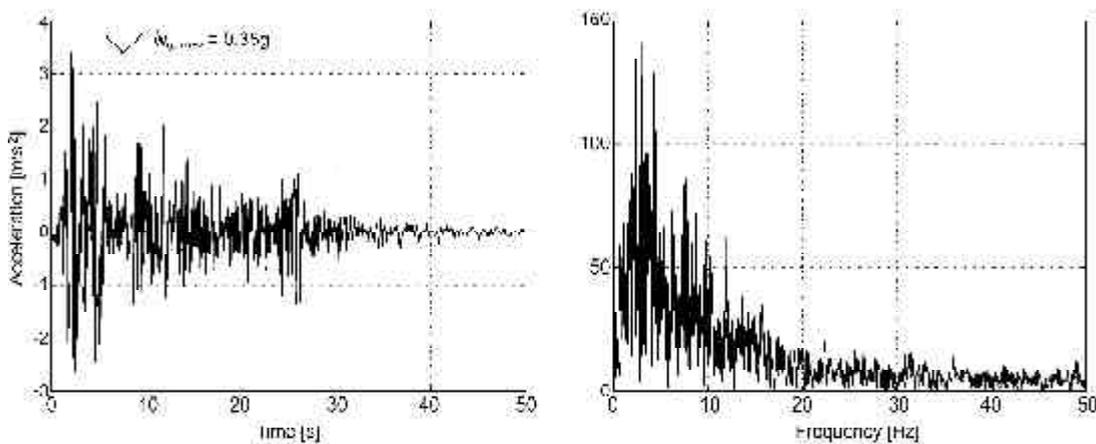
Figure 11. N-S El Centro earthquake in time and frequency domain. Source: University of Notre Dame, http://www.nd.edu/~quake.

The numerically obtained results of the time history response of the main system, with and without two *TLCD* with turbulent damping attached, under combined action of the *N-S* El Centro earthquake are illustrated in Figure (12a). The efficient gain in effective structural vibration, which is solely due to the installation of the two optimally tuned *TLCD*, is seen in Figure (12a) by the large reduction of the maximum vibration amplitudes, also when compared with Figure (10a). Furthermore, Figure (12b) shows no identifiable difference in the time history response of the main system with *TLCD* and turbulent damping, with and without consideration of the vertical excitation, similar to Figure (10b).

In practical applications, Eq. (35) influences the air chamber design twofold: the equilibrium pressure p_0 is assigned and the height H_a is determined. The remaining volume, say A_H (H_a -$2U_{max}$) can be redesigned with a larger cross-sectional area if $H_a > 3U_{max}$. In the model benchmark problem considered above, $H_a \approx 3U_{max}$, leaving the design of the air chambers unchanged.

7. Conclusions

Tuning of the linearized *TLCD* with respect to a selected mode of the main system is simple since a geometric analogy exists to Den Hartog's optimal parameters of a *TMD*. Subsequent fine-tuning in state space is recommended, using the relevant tools of *MATLAB*. The outcome of computer simulations compare well with experimentally derived results if an averaged turbulent damping of the relative fluid motion is considered. Using an air-spring effect in sealed pressurized air chambers can extend the frequency range of application of *TLCD*. For extremely low frequency tuning, the air chambers of the U-shaped piping system remain connected, to allow for a free flow of the air when compressed by the slow fluid motion.

TLCD considerably increase the effective structural damping of "*horizontal*" vibrations, e.g., forced by wind gusts or by the horizontal component of earthquakes. The vertical component of the latter may however produce unwanted parametric excitation of the fluid motion. A detailed study of this effect is performed by computer simulation and verified experimentally. The cut-off value of the equivalent linear damping coefficient of the fluid motion for the most critical case of parametric resonance has been checked experimentally together with the sufficient condition of requiring even higher damping values. If such a condition holds, it was proven that no worsening effect of the resulting effective structural damping is observable under combined seismic loads. In conclusion, under these conditions, the vertical excitation can be neglected at all with respect to the *TLCD*-performance. The air spring effect in sealed *TLCD* reduces the cut-off value of the linear damping coefficient and renders the required insensitivity with the optimal damping applied.

A three story benchmark structure with two sealed *TLCD* in parallel connection, tuned to the basic mode and attached on top, illustrate the benefits of the proposed analysis and confirmed the sufficient condition based on the cut-off damping of parametric resonance. *TLCD* tuned to higher modes can be either

Figure 12. Top floor displacements of the three-DOF-test structure forced by the scaled N-S El Centro seismogram. (a) Bi-axial excitations, identical seismograms applied. Two optimally tuned TLCD in parallel connection (turbulent damping $\rightarrow \delta_{L1} = 0.61=$ constant, $\rightarrow \delta_{L2} = 0.65=$ constant). Note the much higher reduction of the maximum peak, $\approx 40\%$, when compared to Figure (10a). (b) Responses under bi-axial excitations (note the different scale in Figure (12a)) and under uni-axial horizontal excitation. Cut-off damping verified by inspection.

located on top or at the floor of the main structure with maximum drift. An application in combination with base isolation is discussed in Ref. [18]. Damping of long span bridges is considered in Refs. [6] and [19].

Acknowledgement

References

1. Soong, T.T. and Dargush, GF. (1997). "Passive Energy Dissipation Systems in Structural Engineering", John Wiley&Sons, New York.

2. Sakai, F., Takaeda, S., and Tamaki, T. (1989). "Tuned Liquid Column Damper-New Type Device for Suppression of Building Vibrations", *Proc. Conference on High-rise Buildings*, Nanjing, China, 926-931.

3. Hitchcock, P.A., Kwok, K.C.S., Watkins, R.D., and Samali, B. (1997). "Characteristics of Liquid Column Vibration Absorbers (LCVA)-I", *Engineering Structures*, **19**, 126-134.

4. Hitchcock, P.A., Kwok, K.C.S., Watkins, R.D., and Samali, B. (1997). "Characteristics of Liquid Column Vibration Absorbers (LCVA)-II", *Engineering Structures*, **19**, 135-144.

5. Hochrainer, M.J. (2001). "Control of Vibrations of Civil Engineering Structures with Special Emphasis on Tall Buildings", Dissertation (in English), TU-Wien, A-1040 Vienna, Austria.

6. Reiterer, M. (2004). "Damping of Vibration-Prone Civil Engineering Structures with Emphasis on Bridges", Dissertation (in German), TU-Wien, A-1040, Vienna, Austria.

7. Den Hartog, J.P. (1956). "Mechanical Vibrations", Reprint of 4th ed., McGraw-Hill, New York.

8. Ziegler, F. (1998). "Mechanics of Solids and Fluids", 2nd ed., Vienna-New York: Springer Verlag.

9. Spencer, B.F. Jr., Dyke, S.J., Deoskar, H.S. (1997). "Benchmark Problems in Structural Control, Part II: Active Tendon System", In: Proc. of the 1997 ASCE Structures Congress, Portland, Oregon, http://www.nd.edu/~quake.

10. Idelchick, I.E. (1960). "Handbook of Hydraulic Resistance, Coefficient of Local Resistance and of Friction", Available from the U.S. Department of Commerce, Springfield.

11. Clough, R.W. and Penzien, J. (1975). "Dynamic of Structures", McGraw-Hill, New York.

12. Reiterer, M. and Hochrainer, M.J. (2003). "Investigation of Parametric Resonance in Tuned Liquid Column Dampers", PAMM, **3**, 122-123, www.gamm-proceedings.com.

13. Nayfeh, A.H. and Mook, D.T. (1979). "Nonlinear Oscillations", John Wiley & Sons.

14. Klotter, K (1978). "Technische Schwingungs-lehre", **1**, 3rd ed., Berlin: Springer Verlag.

15. Reiterer, M. and Hochrainer, M.J. (2004). "Parametric Resonance in Tuned Liquid Column Dampers: An Experimental Investigation", ÖIAZ - Österreichische Ingenieur und Architektenzeitschrift, (in Press).

16. Yalla, S.K. and Kareem, M. (2000). "On the Beat Phenomenon in Coupled Systems", *Proc. 8th ASCE Specialty Conference on Probabilistic Mechanics and Structural Reliability*, New York, 1-5.

17. Ambraseys, N., Smit, P., Sigbjörnsson, R., Suhadolc, P., and Margaris, B. (2001). "Internet-Site for European Strong-Motion Data", http://www.isesd.cv.ic.ac.uk, European Commission, Directorate-General XII, Environmental and Climate Program, Bruxelles, Belgium.

18. Hochrainer, M and Ziegler, F. (2004). "Tuned Liquid Column Damper-a Cheap Device for Control of Tall Building Vibrations", *Proc. 3rd European Conference on Structural Control,* Schriftenreihe der TU-Wien, (in Press), ISBN-3-901167, S1-179-S1-182.

19. Reiterer, M. (2004). "Control of Pedestrian-Induced Bridge Vibrations by Tuned Liquid Column Dampers", *Proc. 3rd European conf. on Structural Contro*l, Schriftenreihe der TU-Wien, (in Press), ISBN-3-901167, S6-16-S6-19.